Scientific
Research

Mechanisms of Proton-Proton Inelastic Cross-Section Growth in Multi-Peripheral Model within the Framework of Perturbation Theory. Part 2

Igor Sharf[1], Andrii Tykhonov[1,2], Grygorii Sokhrannyi[1], Maksym Deliyergiyev[1,2], Natalia Podolyan[1], Vitaliy Rusov[1,3*]

[1]Department of Theoretical and Experimental Nuclear Physics,
Odessa National Polytechnic University, Shevchenko Odessa, Ukraine
[2]Department of Experimental Particle Physics, Jožef Stefan Institute, Ljubljana, Slovenia
[3]Department of Mathematics, Bielefeld University, Universitatsstrasse Bielefeld, Germany
Email: *siiis@te.net.ua

ABSTRACT

We demonstrate a new technique for calculating proton-proton inelastic cross-section, which allows one by application of the Laplace' method replace the integrand in the integral for the scattering amplitude in the vicinity of the maximum point by expression of Gaussian type. This, in turn, allows us to overcome the computational difficulties for the calculation of the integrals expressing the cross section to sufficiently large numbers of particles. We have managed to overcome these problems in calculating the proton-proton inelastic cross-section for production ($n \leq 8$) number of secondary particles in within the framework of ϕ^3 model. As the result the obtained dependence of inelastic cross-section and total scattering cross-section on the energy $\sqrt{s}$ are qualitative agrees with the experimental data. Such description of total cross-section behavior differs considerably from existing now description, where Reggeons exchange with the intercept greater than unity is considered.

Keywords: Inelastic Scattering Cross-Section; Total Scattering Cross-Section; Laplace Method; Virtuality; Multi-Peripheral Model; Regge Theory

1. Introduction

The problems of the inelastic scattering cross-sections calculation have been discussed in details in [1]. As the result of approximations, which are usually made to overcome these difficulties [2-5], are obtained the integral over the areas of phase space, where different points correspond to different values of the energy-momentum, but at the same time they come to the equation with equal weights. Therefore, the energy-momentum conservation law does not consider reasonably.

Besides, the virtualities, in the equation for the amplitude, reduced to values of the square of transversal components particles momentums [6], meanwhile the rest components of virtualities are not insignificant and appear as quite essential [1].

These approximations are based on the assumption that the main contribution to the integral makes the multi-Regge domain [7]. This assumption is crucial for the modern ap-

proaches to the description of inelastic scattering processes [8]. However, the obtained results in [1] lead to the conclusion that main contribution in the integral does not make the multi-Regge domain.

The aim of this paper is to propose an alternative method for calculating inelastic scattering cross-sections based on well-known Laplace' method for the multidimensional integral [9]. In order to apply this method it is required the element of integration has the point of maximum within integration domain. It has been shown [1] that for the diagrams of "comb" type with the accurate energy-momentum conservation law calculation the square of scattering amplitude module is really has that maximum.

Analysis of the properties of this maximum led to the conclusion that there is the mechanism of cross-section growth. This mechanism has not been considered previously, due to the above approximations associated with the multi-Regge kinematics. Now we would like to show that this mechanism can be responsible for the experimentally observed behavior of cross sections dependence with energy $\sqrt{s}$. However, application of Laplace's me-

---

*Corresponding author.

thod to the processes of production of large number of secondary particles faces the challenge of accounting the vast amount of interference contributions, which will be discussed in detail in Section 3 of this work. In fact, there are $n!$ of these contributions for the process with production of n secondary particles. Therefore, in the present paper we were able to calculate all interference contributions to the production of $n \leq 8$ secondary particles.

Typically, these contributions are underestimate, because according to the considering assumption that particles on the "comb" strongly ordered in rapidity [3] or strongly ordered in Sudakov's parameters [4], they should be negligible.

However, later in this paper, we show that these contributions are significant and the contribution from the square modulus of just one "comb" type diagram with initial particles arrangement, which are usually limited, is only a small fraction of the sums of all interference contributions. Despite the fact that it was possible to calculate the partial cross sections only for small amounts of secondary particles, we can achieve qualitative agreement with experimental results.

2. On the Need of Consideration of Diagrams with the Different Sequence of the Attaching External Lines to the "Comb"

An inelastic scattering cross-section, which is interesting for us, is described by the following equation:

$$\sigma_n = \frac{1}{4n!I} \int \frac{\mathrm{d}\boldsymbol{P}_3}{2P_{30}(2\pi)^3} \frac{\mathrm{d}\boldsymbol{P}_4}{2P_{40}(2\pi)^3} \prod_{k=1}^{n} \frac{\mathrm{d}\boldsymbol{p}_k}{2p_{0k}(2\pi)^3}$$
$$\times \Phi \delta^{(4)}\left(P_3 + P_4 + \sum_{k=1}^{n} p_k - P_1 - P_2\right) \quad (1)$$

where

$$I = \sqrt{\left(P_1 P_2\right)^2 - \left(M_1 M_2\right)^2} \quad (2a)$$

$$\Phi = \left| T\left(n, p_1, p_2, \cdots, p_n, P_1, P_2, P_3, P_4\right) \right|^2 \quad (2b)$$

The scattering amplitude in this equation will be considered within framework of the multi-peripheral model, *i.e.*, for the diagrams of "comb" type. However, here we will make the important remark.

According to the Wick theorem, the scattering amplitude is the sum of diagrams with all possible orders of external lines attaching to the "comb". In the terms of diagram technique it looks as follows. Plotting the multi-peripheral diagram of the scattering amplitude (as it is shown in **Figure 1** of [1]) at first we have adequate number of vertices with three lines going out of it and n lines corresponding to the secondary particles as it is shown in **Figure 1(a)**.

"Pairing" some lines **Figure 1(a)** in order to obtain the "comb", we will get a situation shown in **Figure 1(b)**.

The weighting coefficient appearing from this procedure is included to the coupling constant. Finally we have to "pair" the appropriate lines of particles in the final state with the remaining unpaired internal lines in the diagram of **Figure 1**.

If we marked by i_1—the external line, paired with the first vertex; i_2—the external line, paired with the second vertex and etc.; then i_k is an external line, which is paired with k-th vertex, so every diagram will be characterized by sequence $i_1, i_2, \cdots, i_n$. And in this case the total amplitude is expressed by the sum of $n!$ terms, each of them corresponds to one of $n!$ possible index sequences and therefore the inelastic scattering cross-section can be written as

$$\sigma_n = I' \int \frac{\mathrm{d}\boldsymbol{P}_3}{2P_{30}(2\pi)^3} \frac{\mathrm{d}\boldsymbol{P}_4}{2P_{40}(2\pi)^3} \prod_{k=1}^{n} \frac{\mathrm{d}\boldsymbol{p}_k}{2p_{0k}(2\pi)^3}$$
$$\times \Phi' \delta^{(4)}\left(P_3 + P_4 + \sum_{k=1}^{n} p_k - P_1 - P_2\right) \quad (3)$$

$$I' = \frac{\left(\left(2\pi\right)^4\right)^2 g^4 \lambda^{2n}}{4n!\sqrt{\left(P_1 P_2\right)^2 - \left(M_1 M_2\right)^2}} \quad (4a)$$

$$\Phi' = \left(\sum_{P(i_1, i_2, \cdots, i_n)} A\left(n, P_3, P_4, p_{i_1}, p_{i_2}, \cdots, p_{i_n}, P_2, P_1\right)\right)^*$$
$$\times \left(\sum_{P(j_1, j_2, \cdots, j_n)} A\left(n, P_3, P_4, p_{j_1}, p_{j_2}, \cdots, p_{j_n}, P_2, P_1\right)\right) \quad (4b)$$

Here, as well as in [1], M_1 and M_2 are the masses of particles in initial state and we assume that $M_1 = M_2 = M$, where M is proton mass. Moreover, P_1 and P_2 are four-momenta of initial protons; P_3 and P_4 are four-momenta of protons in the finite state; p_k, $k = 1, 2, \cdots, n$ are four-momenta of secondary particles (pions of mass m). As the virtual particles we understand the quanta of real scalar field with pion mass m. A coupling
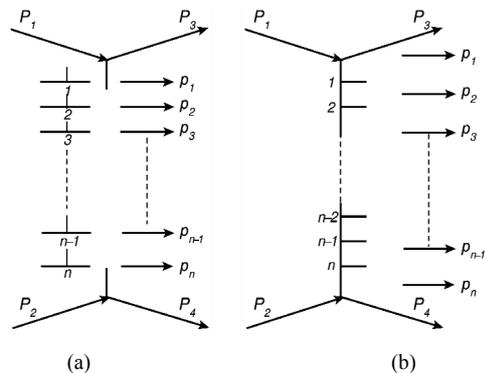

Figure 1. Plotting diagrams of the "comb" type.

constant in vertexes, in which the pion lines join with proton lines, is denote as g and λ is coupling constant in vertexes, where three pion lines meet. The function A is defined by:

$$
\begin{aligned}
& A\left(n, P_3, P_4, p_1, p_2, \cdots, p_n, P_1, P_2\right) \\
& = \frac{1}{m^2 - \left(P_1 - P_3\right)^2 - i\varepsilon} \times \frac{1}{m^2 - \left(P_1 - P_3 - p_1\right)^2 - i\varepsilon} \\
& \times \frac{1}{m^2 - \left(P_1 - P_3 - p_1 - p_2\right)^2 - i\varepsilon} \\
& \times \frac{1}{m^2 - \left(P_1 - P_3 - p_1 - p_2 - \cdots - p_{n-1}\right)^2 - i\varepsilon} \\
& \times \frac{1}{m^2 - \left(P_1 - P_3 - p_1 - p_2 - \cdots - p_{n-1} - p_n\right)^2 - i\varepsilon}
\end{aligned}
\tag{5}
$$

Moreover, as it was shown in [1], the function A is real and positive therefore sign of complex conjugation in Equation (3) can be dropped and we can rewrite this expression in the following form:

$$
\begin{aligned}
\sigma_n = I' \sum_{\substack{P(i_1, i_2, \cdots, i_n) \\ P(j_1, j_2, \cdots, j_n)}} & \int \frac{\mathrm{d}P_3}{2P_{30}(2\pi)^3} \frac{\mathrm{d}P_4}{2P_{40}(2\pi)^3} \prod_{k=1}^{n} \frac{\mathrm{d}p_k}{2p_{0k}(2\pi)^3} \\
& \times \delta^{(4)}\left(P_3 + P_4 + \sum_{k=1}^{n} p_k - P_1 - P_2\right) \\
& \times A\left(n, P_3, P_4, p_{i_1}, p_{i_2}, \cdots, p_{i_n}, P_2, P_1\right) \\
& \times A\left(n, P_3, P_4, p_{j_1}, p_{j_2}, \cdots, p_{j_n}, P_2, P_1\right)
\end{aligned}
\tag{6}
$$

where I' defined by Equation (4a).

Notation $\displaystyle\sum_{P(i_1, i_2, \cdots, i_n)}$ means that we consider sum of terms corresponding to all possible permutations of indices $i_1, i_2, \cdots, i_n$. Let us note that the integration variables in each of term of considered sum can be renaming, so that the indexes $i_1, i_2, \cdots, i_n$ formed the original placing $1, 2, \cdots, n$. At the same time the indexes $j_1, j_2, ..., j_n$ will run through all possible permutations and summation must be carried over all these permutations. Taking into account this, we get instead of Equation (6):

$$
\begin{aligned}
\sigma_n = I'' \int & \frac{\mathrm{d}P_3}{2P_{30}(2\pi)^3} \frac{\mathrm{d}P_4}{2P_{40}(2\pi)^3} \prod_{k=1}^{n} \frac{\mathrm{d}p_k}{2p_{0k}(2\pi)^3} \\
& \times \delta^{(4)}\left(P_3 + P_4 + \sum_{k=1}^{n} p_k - P_1 - P_2\right) \\
& \times \Phi\left(n, P_3, P_4, p_1, p_2, \cdots, p_n, P_2, P_1\right)
\end{aligned}
\tag{7}
$$

where

$$
I'' = \frac{\left(\left(2\pi\right)^4\right)^2 g^4 \lambda^{2n}}{4n\sqrt{s/4 - \left(M_1 M_2\right)^2}\sqrt{s}}
\tag{8}
$$

$$
\begin{aligned}
& \Phi\left(n, P_3, P_4, p_1, p_2, \cdots, p_n, P_2, P_1\right) \\
& = A\left(n, P_3, P_4, p_2, p_1, \cdots, p_n, P_2, P_1\right) \\
& \times \sum_{P(j_1, j_2, \cdots, j_n)} A\left(n, P_3, P_4, p_{j_1}, p_{j_2}, \cdots, p_{j_n}, P_2, P_1\right)
\end{aligned}
\tag{9}
$$

Now we can use the fact that the amplitudes A in Equation (9) have the points of constrained maximum [1].

3. Computation of Contributions to Inelastic Scattering Cross-Sections Corresponding to the Multi-Peripheral Diagrams by Laplace Method

For further analysis, we examine expression Equation (6) in c.m.s. separating the longitudinal and transverse to the collision axis components of three-dimensional particle momenta

$$
\begin{aligned}
\sigma_n = I'' \int & \frac{\mathrm{d}\boldsymbol{P}_{3\perp}\mathrm{d}P_{3\|}}{2(2\pi)^3\sqrt{M^2 + P_{3\|}^2 + \boldsymbol{P}_{3\perp}^2}} \frac{\mathrm{d}\boldsymbol{P}_{4\perp}\mathrm{d}P_{4\|}}{2(2\pi)^3\sqrt{M^2 + P_{4\|}^2 + \boldsymbol{P}_{4\perp}^2}} \\
& \times \prod_{k=1}^{n} \frac{\mathrm{d}\boldsymbol{p}_{k\perp}\mathrm{d}p_{k\|}}{2\sqrt{m + p_{k\|}^2 + \boldsymbol{p}_{k\perp}^2}(2\pi)^3} \\
& \times \Phi\left(n, p_{1\|}, \boldsymbol{p}_{1\perp}, p_{2\|}, \boldsymbol{p}_{2\perp}, \cdots,\right. \\
& \qquad \left. p_{n\|}, \boldsymbol{p}_{n\perp}, P_{1\|}, P_{2\|}, P_{3\|}, \boldsymbol{P}_{3\perp}, P_{4\|}, \boldsymbol{P}_{4\perp}\right) \\
& \times \delta\left(T_3 + T_4 + \sum_{k=1}^{n} \sqrt{1 + p_{3\|}^2 + \boldsymbol{p}_{3\perp}^2} - \sqrt{s}\right) \\
& \times \delta\left(\sum_{k=1}^{n} p_{k\|} + P_{3\|} + P_{4\|}\right)\delta\left(\sum_{k=1}^{n} p_{k\perp x} + P_{3\perp x} + P_{4\perp x}\right) \\
& \times \delta\left(\sum_{k=1}^{n} p_{k\perp y} + P_{3\perp y} + P_{4\perp y}\right)
\end{aligned}
\tag{10}
$$

where I'' defined by Equation (8) and

$$
T_3 = \sqrt{M^2 + P_{3\|}^2 + \boldsymbol{P}_{3\perp}^2}
\tag{11a}
$$

$$
T_4 = \sqrt{M^2 + P_{4\|}^2 + \boldsymbol{P}_{4\perp}^2}
\tag{11b}
$$

The last three δ-functions in Equation (10), whose arguments are linear with respect to integration variables, we can vanish by the integration over $P_{4\|}$, $P_{4\perp x}$, $P_{4\perp y}$. In order to take into account the rest δ-function, which expresses the energy conservation law let's replace $P_{3\|}$ by new integration variable

$$E_p = \sqrt{M^2 + P_{3\parallel}^2 + \boldsymbol{P}_{3\perp}^2}$$
$$+ \sqrt{M^2 + \left(\sum_{k=1}^{n} p_{k\parallel} + P_{3\parallel}\right)^2 + \left(\sum_{k=1}^{n} \boldsymbol{p}_{k\perp} + \boldsymbol{P}_{3\perp}\right)^2} \quad (12)$$

Those, making the following replacement we must express $P_{3\parallel}$ through E_p. The corresponding expression will coincide with Equation (8) in [1] with the positive sign in front of the square root. Moreover, introduce the rapidities instead of longitudinal momenta:

$$p_{k\parallel} = m_\perp(\boldsymbol{p}_{k\perp})\operatorname{sh}(y_k) \quad (13a)$$

$$m_\perp(\boldsymbol{p}_{k\perp}) = \sqrt{m + \boldsymbol{p}_{k\perp}^2} \quad (13b)$$

After these transformations we get:

$$\sigma_n = \frac{(2\pi)^2 g^4 \lambda^{2n}}{4\sqrt{s/4 - M^2}\sqrt{s}} \int \frac{\mathrm{d}\boldsymbol{P}_{3\perp}}{2\sqrt{M^2 + P_{3\parallel}^2 + \boldsymbol{P}_{3\perp}^2}}$$
$$\times \prod_{k=1}^{n} \frac{\mathrm{d}\boldsymbol{p}_{k\perp}\mathrm{d}y_{k\parallel}}{2(2\pi)^3} \frac{\partial P_{3\parallel}}{\partial E_p}\bigg|_{E_p = \sqrt{s} - \sum_{k=1}^{n} m_{\perp k}(\boldsymbol{p}_{\perp k})\operatorname{ch}(y_k)} \quad (14)$$
$$\times \frac{\Phi'}{2\sqrt{M^2 + \left(\sum_{k=1}^{n} p_{k\parallel} + P_{3\parallel}\right)^2 + \left(\sum_{k=1}^{n} \boldsymbol{p}_{k\perp} + \boldsymbol{P}_{3\perp}\right)^2}}$$

where

$$\Phi' = \Phi\big(n, y_1, \boldsymbol{p}_{1\perp}, y_2, \boldsymbol{p}_{2\perp}, \cdots,$$
$$y_n, \boldsymbol{p}_{n\perp}, P_{1\parallel}, P_{2\parallel}, P_{3\parallel}, \boldsymbol{P}_{3\perp}, P_{4\parallel}', \boldsymbol{P}_{4\perp}'\big) \quad (15)$$

with

$$P_{4\parallel}' = -\left(\sum_{k=1}^{n} m_\perp(\boldsymbol{p}_{k\perp})\operatorname{sh}(y_k) + P_{3\parallel}\right) \quad (16a)$$

$$\boldsymbol{P}_{4\perp}' = -\left(\sum_{k=1}^{n} \boldsymbol{p}_{k\perp} + \boldsymbol{P}_{3\perp}\right) \quad (16b)$$

Note that the $P_{3\parallel}$ is expressed through the other variables of integration by Equation (8) in [1].

Now turn to the dimensionless integration variables and made the following replacement $\boldsymbol{p}_{k\perp} \rightarrow \boldsymbol{p}_{k\perp}/m$, $\boldsymbol{P}_{3\perp} \rightarrow \boldsymbol{P}_{3\perp}/m$. We designate the new dimensionless integration variables just as the old variables, for short. Moreover, replace expression for $P_{3\parallel}$ by the same expression divided by m. The same concerns the constants in expressions for cross-section, *i.e.*, the designations M and $\sqrt{s}$ are used for proton mass and energy of colliding particles in c.m.s., which is made dimensionless with the pion mass m.

Now introduce the following notations of integration variables in Equation (14) and designate the rapidities $y_1, y_2, \cdots, y_n$ as $X_1, X_2, \cdots, X_n$; x-components of transverse momenta of secondary particles $p_{1\perp x}, p_{2\perp x}, \cdots, p_{n\perp x}$ as $X_{n+1}, X_{n+2}, \cdots, X_{2n}$; y-components of transverse momenta of secondary $p_{1\perp y}, p_{2\perp y}, \cdots, p_{n\perp y}$ as

$X_{2n+1}, X_{2n+2}, \cdots, X_{3n}$. Moreover, designate X_{3n+1} as $P_{3\perp x}$ and X_{3n+2} as $P_{3\perp y}$.

As it was shown in the previous sections, that an integrand $A(n, P_3, P_4, p_1, p_2, \cdots, p_n, P_2, P_1)$ in Equation (14), expressed as a function of independent integration variables, has a maximum point in the domain of integration. At the neighborhood of this maximum point it can be represented in the form

$$A(n, P_3, P_4, p_1, p_2, \cdots, p_n, P_2, P_1)$$
$$= A^{(0),n}(\sqrt{s}) \quad (17)$$
$$\times \exp\left(-\frac{1}{2}\sum_{a=1}^{3n+2}\sum_{b=1}^{3n+2} D_{ab}\left(X_a - X_a^{(0)}\right)\left(X_b - X_b^{(0)}\right)\right)$$

where $A^{(0),n}(\sqrt{s})$ is the value of function (see Equation (4) in [1]) at the point of constrained maximum; $D_{ab} = \dfrac{\partial^2}{\partial X_a \partial X_b}$, where derivatives are taken at the constrained maximum point of scattering amplitude; $X_a^{(0)}$-value of variables, maximize the scattering amplitude. That is, the real and positive value A defined by Equation (4) (see [1]) is represented as $A = \exp(\ln(A))$, and exponential function is expanded into the Taylor series in the neighborhood of the maximum point with an accuracy up to the second-order summands.

An accuracy of approximation Equation (17) can be numerically verified in the following way. Function A, defined by Equation (4) (see [1]) can be written as

$$A = A(n, X_1, X_2, \cdots, X_{3n+2}) \quad (18)$$

Let us introduce also the notation:

$$A^{(g)}(n, X_1, X_2, \cdots, X_{3n+2})$$
$$= A^{(0),n}(\sqrt{s})\exp\left(-\frac{1}{2}\sum_{a=1}^{3n+2}\sum_{b=1}^{3n+2} D_{ab}\left(X_a - X_a^{(0)}\right)\left(X_b - X_b^{(0)}\right)\right)$$
$$(19)$$

Now let us examine functions:

$$F_{ik}^n(a, b)$$
$$= A\left(n, X_1^{(0)}, X_2^{(0)}, \cdots, X_i^{(0)} + a, \cdots, X_k^{(0)} + b, \cdots, X_{3n+2}^{(0)}\right)$$
$$(20)$$

$$F_{ik}^{(g),n}(a, b)$$
$$= A^{(g)}\left(n, X_1^{(0)}, X_2^{(0)}, \cdots, X_i^{(0)} + a, \cdots, X_k^{(0)} + b, \cdots, X_{3n+2}^{(0)}\right)$$
$$(21)$$

Three-dimensional curves of these functions can be easily plotted in the vicinity of the maximum point (*i.e.*, at the neighborhood of zero of variables a and b). The typical examples of such curves are shown in **Figure 2** and **Figure 3**, where it is easy to see that the approximation Equation (19) works well in the wide energy range. The results similar to ones in **Figures 2-3** were obtained
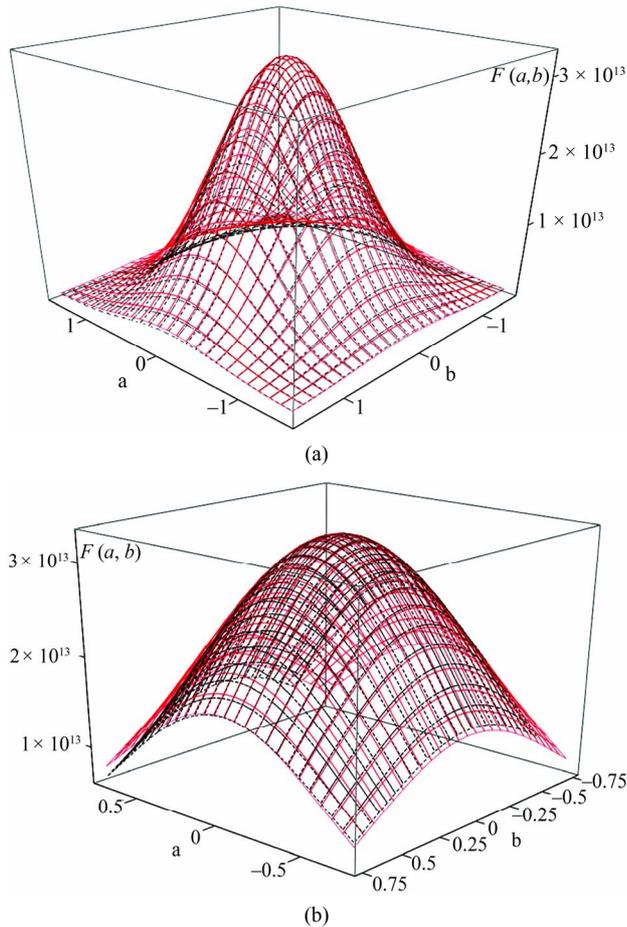
Figure 2. Function $F_{1,7}^{n=10}(a,b)$ (dashed line) and $F_{1,7}^{(g)}(a,b)$ (solid line) at energy $\sqrt{s}$ = 5 GeV and n = 10. The general image 2(a), and the zoomed image 2(b) at the neighborhood of maximum point. Clear that in an area that makes the most significant contribution to the integral, the scattering amplitude does not differ from its Gaussian approximation Equation (19), which demonstrates the possibility of applying the Laplace method.

Figure 3. Function $F_{1,7}^{n=10}(a,b)$ (dashed line) and $F_{1,7}^{(g)}(a,b)$ (solid line) at energy $\sqrt{s}$ = 100 GeV and n = 10. The general image 2(a), and the zoomed image 2(b) at the neighborhood of maximum point. Clear that in an area that makes the most significant contribution to the integral, the scattering amplitude does not differ from its Gaussian approximation Equation (19), which demonstrates the possibility of applying the Laplace method.

at different values of $\sqrt{s}$, i, k and n. As one can see from **Figure 2** and **Figure 3**, that true amplitude and its Gaussian approximation Equation (19) start differ visibly only in the parameter region, which makes a insignificant contribution to the integral.

Now let us proceed with identification $A(n, P_3, P_4, p_1, p_2, \cdots, p_n, P_2, P_1)$ in Equation (9) and define all possible arrangements of indices $1, 2, \cdots, n$ by $P^{(1)}, P^{(2)}, \cdots, P^{(n!)}$. The function of variables X_k, where $k = 1, 2, \cdots, 3n+2$, which corresponds to arrangement $P^{(l)}$, define as $A_{P^{(l)}}(n, X_1, X_2, \cdots, X_{3n+2})$. It differs from the function Equation (18) just by renaming the arguments, and therefore it also has a point of constrained maximum under condition of the energy-momentum conservation. The value of this function at the constrained maximum point is equal to the value of function Equation (18), *i.e.*,
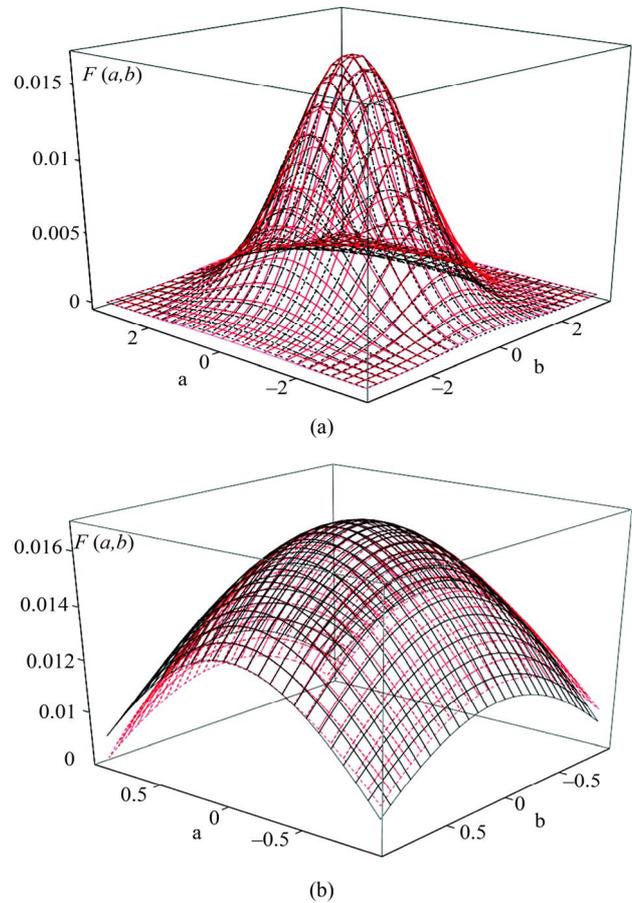
and it is equal to $A^{(0),n}(\sqrt{s})$ according to the replacement made above. Thus, if $X_1^{(0)}, X_2^{(2)}, \cdots, X_n^{(0)}$ are the values of variables $X_1, X_2, \cdots, X_n$ at the maximum point, now same values $X_1^{(0)}, X_2^{(2)}, \cdots, X_n^{(0)}$ will be the values of the variables $X_{j_1}, X_{j_2}, \cdots, X_{j_n}$ at the maximum point. Analogously $X_{n+1}^{(0)}, X_{n+2}^{(2)}, \cdots, X_{2n}^{(0)}$ are the values of variables $X_{n+j_1}, X_{n+j_2}, \cdots, X_{n+j_n}$ at the maximum point, and $X_{2n+1}^{(0)}, X_{2n+2}^{(2)}, \cdots, X_{3n}^{(0)}$ for $X_{2n+j_1}, X_{2n+j_2}, \cdots, X_{3n+j_n}$. For short we label the index of variable, into which the variable a goes at given rearrangement, as $P^{(i)}(a)$ *i.e.*, the variable X_a replaced by the variable $X_{p^{(l)}}(a)$.

If we denote the matrix of second derivatives of the logarithm of the function $A_{p^{(l)}}$ at the maximum point by

$\hat{D}^{P^{(l)}}$, we will get the following approximation for the function $A_{P^{(l)}}$:

$$A_{P^{(l)}}\left(n, X_1, X_2, \cdots, X_{3n+2}\right) = A^{(0),n}\left(\sqrt{s}\right)\exp\left(-\frac{1}{2}K\right) \quad (22)$$

where

$$K = \sum_{a=1}^{3n+2}\sum_{b=1}^{3n+2} D^{P^{(l)}}_{P^{(l)}(a),P^{(l)}(b)}\left(X_{P^{(l)}(a)} - X_a^{(0)}\right)\left(X_{P^{(l)}(b)} - X_b^{(0)}\right) \quad (23)$$

Taking into account that Equation (22) depends on variables $X_{P^{(l)}(a)}$ and $X_{P^{(l)}(b)}$ just as a function A depends on variables X_a and X_b and the second derivative is taken at the same values of arguments, we have

$$D^{P^{(l)}}_{P^{(l)}(a),P^{(l)}(b)} = D_{ab} \quad (24)$$

Using Equation (24) rewrite Equation (22) in more convenient form. For this purpose introduce the matrices $\hat{P}^{(l)}$, $l = 1, 2, \cdots, n!$ and by multiplying it with the column $\hat{X}$ of initial variables in Equation (19), we get a column in which the variables are arranged in that way so that in place of variable X_a became a variable $X_{P^{(l)}(a)}$. At next iteration taking into account Equation (24) one can rewrite Equation (22) in a matrix form in the following way:

$$A_{P^{(l)}}\left(n, X_1, X_2, \cdots, X_{3n+2}\right)$$
$$= A^{(0),n}\left(\sqrt{s}\right)$$
$$\times\exp\left(-\frac{1}{2}\left(\hat{X}^T\left(\hat{P}^{(l)}\right)^T\hat{D}\hat{P}^{(l)}\hat{X} - 2\left(\hat{X}^{(0)}\right)^T\hat{D}\hat{P}^{(l)}\hat{X}\right)\right)$$
$$\times\exp\left(-\frac{1}{2}\left(\left(\hat{X}^{(0)}\right)^T\hat{D}\hat{X}^{(0)}\right)\right) \quad (25)$$

where $\hat{X}^{(0)}$ is a column whose elements are the numbers $X_a^{(0)}$, $a = 1, 2, \cdots, 3n+2$ in the initial arrangement. And now we can rewrite Equation (9) in the form:

$$\Phi\left(n, P_3, P_4, p_1, p_2, \cdots, p_n, P_2, P_1\right)$$
$$= \Phi\left(n, X_1, X_2, \cdots, X_{3n+2}\right)$$
$$= \left(A^{(0),n}\left(\sqrt{s}\right)\right)^2\exp\left(-\left(\hat{X}^{(0)}\right)^T\hat{D}\hat{X}^{(0)}\right) \quad 6$$
$$\times\sum_{l=1}^{n!}\exp\left(-\frac{1}{2}\hat{X}^T\hat{D}^{(l)}\hat{X} + \left(\hat{X}^{(0)}\right)^T\hat{V}^{(l)}\hat{X}\right)$$

where

$$\hat{D}^{(l)} = \hat{D} + \left(\hat{P}^{(l)}\right)^T\hat{D}\hat{P}^{(l)} \quad (27a)$$

$$\hat{V}^{(l)} = \hat{D} + \hat{D}\hat{P}^{(l)} \quad (27b)$$

If now we take up the further consideration of Equation (14), we can see that all the other coefficients (except Φ') under the integral don't change the values under the permutation of arguments. We replace these expressions by their values at the maximum point and take

them out from integral. From this, we introduce the following notation:

$$J^{(0),n}\left(\sqrt{s}\right) = \left.\frac{\partial P_{3\parallel}^{(0)}}{\partial E_p}\right|_{E_p=\sqrt{s}-\sum_{k=1}^{n}\mathrm{ch}\left(y_k^{(0)}\right)} \quad (28)$$

where $P_{3\parallel}^{(0)}$ is the value of expression (see Equation 8 in [1]), corresponding to particle momenta, for which the scattering amplitude has maximum, *i.e.*, at the $X_a^{(0)}$ and undimensionalized by m.

The expression for cross-section in this case can be written in the form:

$$\sigma_n = \frac{(2\pi)^2}{16m^2\sqrt{s/4-M^2}\sqrt{s}\sqrt{M^2+\left(P_{3\parallel}^{(0)}\right)^2}}$$
$$\times\frac{(2\pi)^2}{\sqrt{M^2+\left(\sum_{k=1}^{n}\mathrm{sh}\left(y_k^{(0)}\right)+P_{3\parallel}^{(0)}\right)^2}}\left(\frac{g}{m}\right)^4\left(\frac{1}{2(2\pi)^3}\left(\frac{\lambda}{m}\right)^2\right)^n$$
$$\times\left(A^{(0),n}\left(\sqrt{s}\right)\right)^2 J^{(0),n}\left(\sqrt{s}\right)\exp\left(-\left(\hat{X}^{(0)}\right)^T\hat{D}\hat{X}^{(0)}\right)$$
$$\sum_{l=1}^{n!}\int\prod_{k=1}^{3n+2}\mathrm{d}X_a\exp\left(-\frac{1}{2}\hat{X}^T\hat{D}^{(l)}\hat{X} + \left(\hat{X}^{(0)}\right)^T\hat{V}^{(l)}\hat{X}\right) \quad (29)$$

As the value $\sum_{k=1}^{n}sh\left(y_k^{(0)}\right)+P_{3\parallel}^{(0)}$ in Equation (29) is the negative value of longitudinal component of momentum $P_{4\parallel}^{(0)}$ taken at the maximum point, it can be replaced by $P_{3\parallel}^{(0)}$ due to the symmetry properties that have been discussed above.

Multidimensional integrals under the summation sign can be calculated by diagonalizing of quadratic form in the exponent of each of them. Such diagonalization can be numerical realized, for instance, by the Lagrange method. The large number of terms in Equation (29) is substantial computational difficulty, which we overcame only for the number of particles $n \le 8$. To represent results of numerical computations, it is useful to decompose Equation (29) in the following way:

$$f_P^{(n)}\left(\sqrt{s}\right)$$
$$= \exp\left(-\left(\hat{X}^{(0)}\right)^T\hat{D}\hat{X}^{(0)}\right) \quad (30)$$
$$\times\sum_{l=1}^{n!}\int\prod_{k=1}^{3n+2}\mathrm{d}X_a\exp\left(-\frac{1}{2}\hat{X}^T\hat{D}^{(l)}\hat{X} + \left(\hat{X}^{(0)}\right)^T\hat{V}^{(l)}\hat{X}\right)$$

$$\sigma_n'\left(\sqrt{s}\right) = \frac{\left(A^{(0),n}\left(\sqrt{s}\right)\right)^2 J^{(0),n}\left(\sqrt{s}\right)f_P^{(n)}\left(\sqrt{s}\right)}{\sqrt{s/4-M^2}\sqrt{s}\left(M^2+\left(P_{3\parallel}^{(0)}\right)^2\right)} \quad (31)$$

$$L = \frac{1}{2(2\pi)^3}\left(\frac{\lambda}{m}\right)^2 \quad (32)$$

Note, that here and in the following sections we will use the "prime" sign in ours notation to indicate that we use a dimensionless quantity that characterized the dependence of the cross-sections on energy, but not their absolute values.

The Equation (31) differs from the inelastic scattering cross-section $\sigma'_n(\sqrt{s})$ only by the absence of factor $\frac{(2\pi)^2}{16m^2}\left(\frac{g}{m}\right)^2\left(\frac{1}{2(2\pi)^3}\left(\frac{\lambda}{m}\right)^2\right)^n$, which is energy independent and its consideration allow us to trace the dependence of inelastic scattering cross-section on energy $\sqrt{s}$ (**Figures 4-5**).

From **Figure 4** it is obvious that derivatives of cross-sections with respect to energies along the real axis are equal to zero at points corresponding to the threshold energy of *n* particle production, *i.e.*, though the threshold values of energy are branch points for the cross-sections, they have continuous first derivative along the real axis at the branch points. This can be illustrated in the following way.

In the examined approximation of equal denominators, for the even number of particles value of square of scattering amplitude at the maximum point can be written like:

$$\left(A^{(0),n}\right)^2 = \left(1 + \frac{1}{\text{sh}^2\left(y_{n/2}\right)}\right)^{-2(n+1)} \tag{33}$$

where $y_{n/2}$ defined by (see [1]):

$$y_{n/2} = \frac{1}{n+1}\text{arccosh}\left(\frac{\sqrt{s}-n}{2M}\right) \tag{34}$$

Derivative from Equation (34) along the real axis at the threshold branching-point is infinite. However, cause at this point value of $y_{n/2}$ is zero, than from Equation (33) it is obvious that derivative of $A^{(0),n}$ will be converge to threshold along the real axis tends to zero.

As it follows from **Figures 4-5**, $\sigma'_8(\sqrt{s})$ monotone increases in the all considered energy range. At the same time from **Figure 6** one can see that $f_P^{(8)}(\sqrt{s})$ has drop-down sections. Moreover, even on those sections, where $f_P^{(n)}(\sqrt{s})$, $n = 2 \div 5$ increase, corresponding $\sigma'_n(\sqrt{s})$ decrease. It makes possible to conclude, that amplitude growth at maximum point (which is the consequence of virtuality reduction) is generally responsible for the growth of inelastic scattering cross-section.

As it evident from **Figures 4-5** for some values of energy Equation (31) has a positive energy derivative and for some values of energy Equation (31) has a negative energy derivative. This makes a question? If we form from them a quantities

$$\sigma'^{\Sigma}\left(\sqrt{s}\right) = \sum_{n=0}^{8} L^n \sigma'_n\left(\sqrt{s}\right) \tag{35}$$
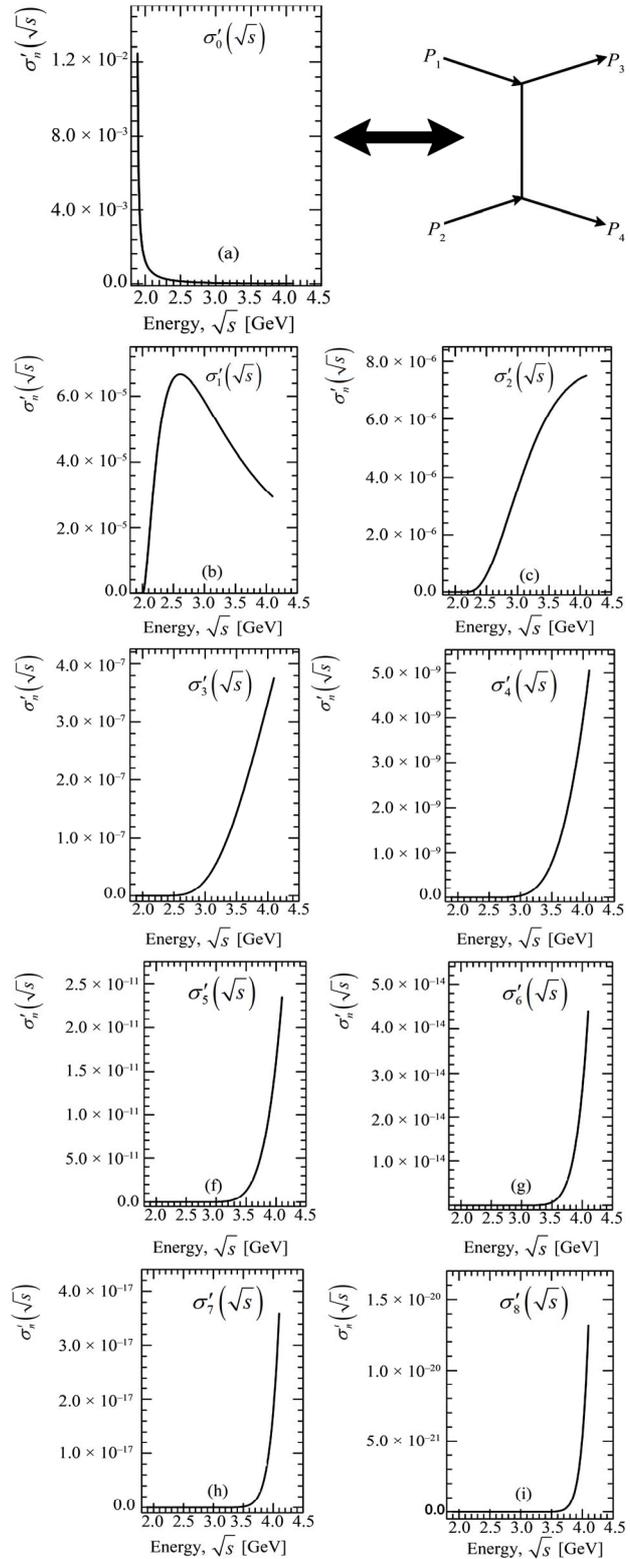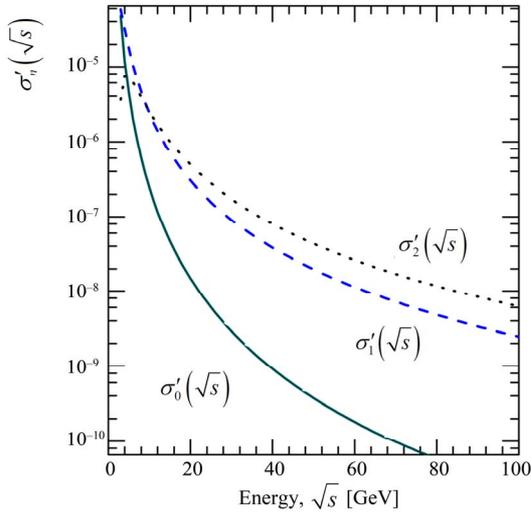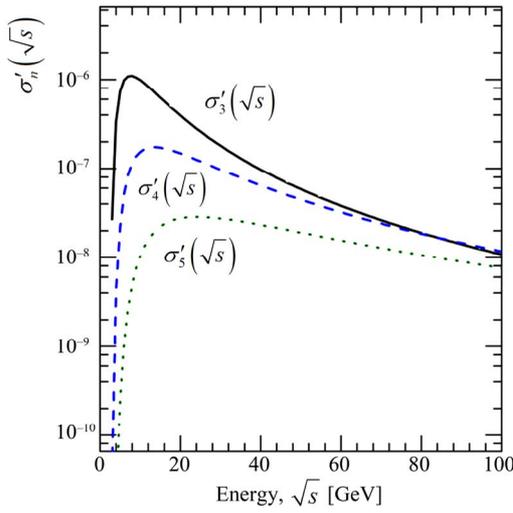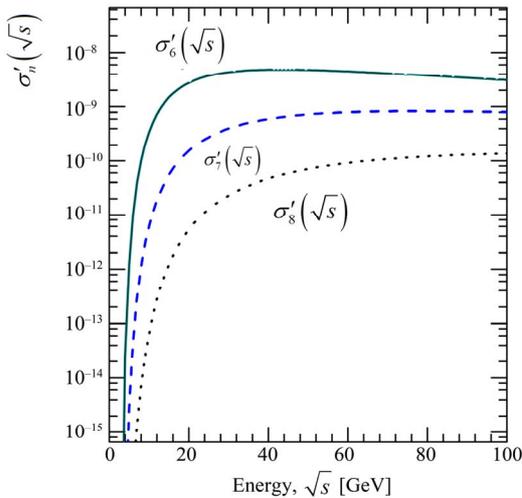

Figure 4. The calculated values of $\sigma'_n(\sqrt{s})$, $n = 0, 1, \cdots, 8$ in the range of threshold energies for 1, 2, $\cdots$, 8 particle productions. Via $\sigma'_0(\sqrt{s})$ was denoted one of the contributions from the diagram (shown on the right) to inelastic scattering cross-section.

(a)

(b)

(c)

Figure 5. Values of $\sigma'_n\left(\sqrt{s}\right)$ in the energy range $\sqrt{s}$ = 3 - 95 GeV.
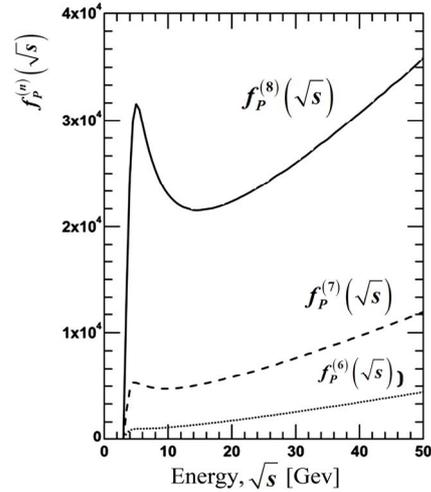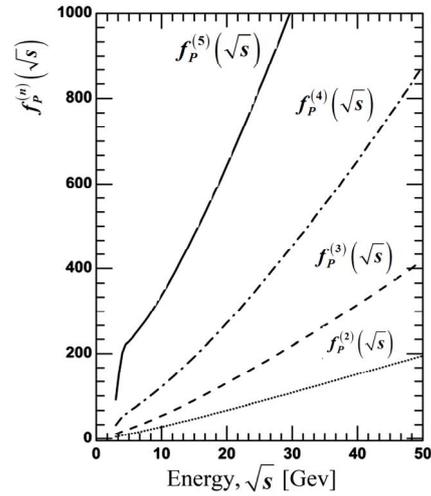

Figure 6. The calculated values of $f_P^{(n)}\left(\sqrt{s}\right)$ determined by Equation (30), in the energy range $\sqrt{s}$ = 3 - 95 GeV.

$$\sigma'^I\left(\sqrt{s}\right) = \sum_{n=1}^{8} L^n \sigma'_n\left(\sqrt{s}\right) \qquad (36)$$

where L is defined by Equation (32), is it possible to choose the "coupling constant" L so that the value of Equation (35) has a characteristic minimum for the total proton-proton scattering cross-section? Answer for this question is positive (see **Figure 7**), *i.e.*, the curves agree qualitatively at the close values of L. The energy range shown in **Figure 7** takes into account all the inelastic contributions. We find indeed very interesting result that curves presented on **Figures 7-8**, where calculated values of Equations (35), (36) are given at $L = 5.57$, qualitatively agree with experimental data [10,11].

Let us point to the fact that in **Figures 7-8** the minimum at higher energies $\sqrt{s}$ than in the experiment. We believe that the accounting contributions with higher number of secondary particles n to $\sigma'_n\left(\sqrt{s}\right)$ and the
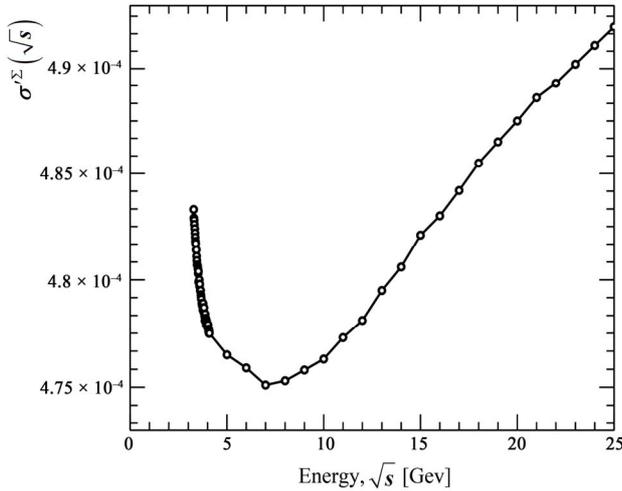
Figure 7. Calculated values of $\sigma'^{\Sigma}\left(\sqrt{s}\right)$ at $L = 5.57$, in the energy range $\sqrt{s} = 5$ - 25 GeV.
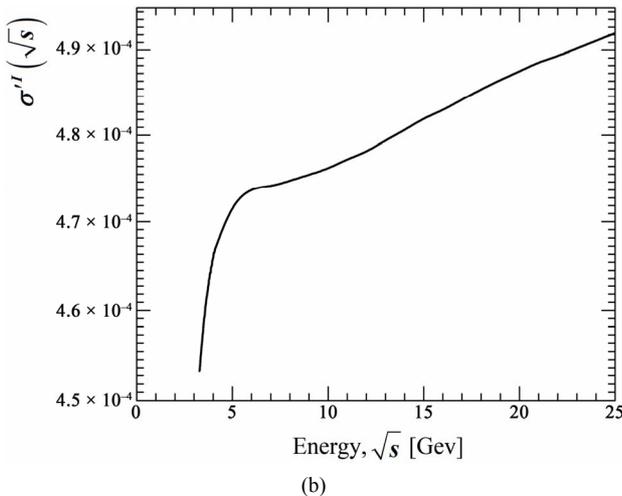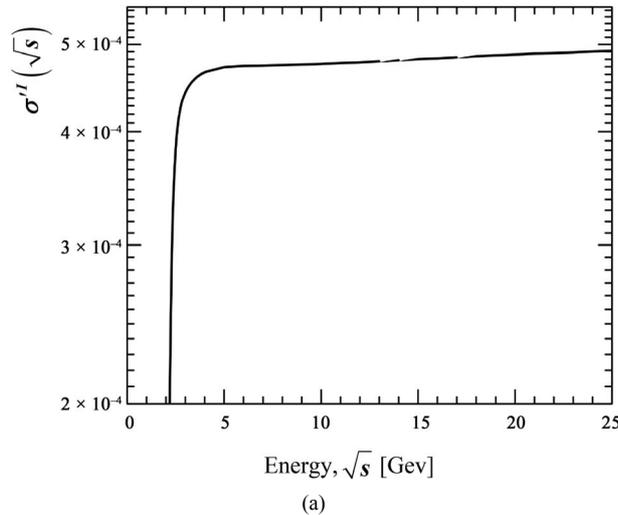

(a)

(b)

Figure 8. Calculated values of $\sigma'^{I}\left(\sqrt{s}\right)$ at $L = 5.57$, in the energy range: (a) $\sqrt{s} = 1.89$ - 25 GeV and (b) $\sqrt{s} = 3$ - 25 GeV.

corresponding change of constant L will "move" a maximum to a required area.

Moreover, in this paper we have examined the simplest diagrams of ϕ^3 theory and we intend to compare the qualitative form of these cross-sections with experimental data, but do not claim quantitative agreement. It is possible to hope that the application of similar computation method to more complicated diagrams in more realistic models will lead to correct outcome.

As known, within the framework of Reggeon theory the drop-down part of total cross-section is described by the Reggeons exchanges with interception less than unity [12,13]. The cuts concerned with multi-Reggeon exchanges with participation of Reggeons with intercept greater than unity are responsible for the cross-section growth after the reaching the minimum [5].

As will be shown further, the accounting of $\sigma'_n\left(\sqrt{s}\right)$ at $n > 8$ will not change the behavior of function $\sigma'^{\Sigma}\left(\sqrt{s}\right)$ Equation (35). This means that within the framework of given model the summation of multi-peripheral diagrams, when we compute the imaginary part of elastic scattering amplitude, will not result in power dependence on energy, since this dependence is monotonic. This, in turn, will mean that the appropriate partial amplitude has no pole singularity! And this obviously differs from the results of standard approach in calculations of multi-peripheral model and from the results of Reggeon theory (see f.ex. [2]).

Another argument in favor of this hypothesis are the results of the "multiplicity distribution" shown in **Figure 9**, where axis of ordinates designates the number of particles n and abscissa axis designates the value of:

$$p_n = \frac{L^n \sigma'_n\left(\sqrt{s}\right)}{\sigma'^I\left(\sqrt{s}\right)} \qquad (37)$$
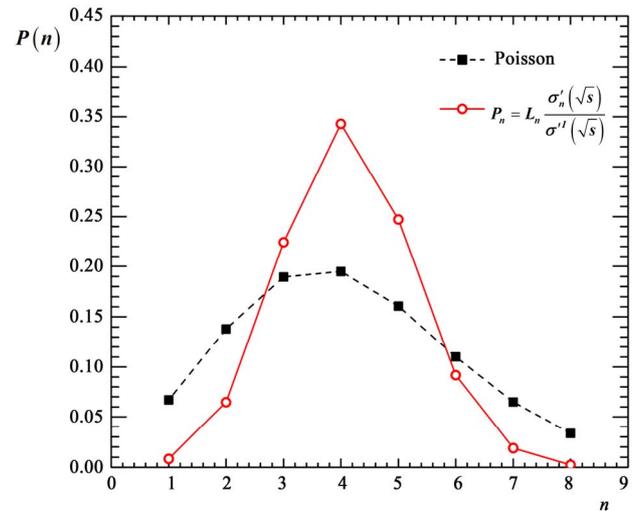

Figure 9. Distribution (see Equation (37)) (red line) and Poisson distribution (dotted line) at $\sqrt{s} = 15$ GeV.

The Poisson distribution for the same average like for distribution Equation (37) is given for comparison. The energy $\sqrt{s}$ = 15 GeV is chosen for example, because at higher energies all distributions is no longer fit in the range from 0 to 8 particles. As is obvious from **Figure 9**, the distribution Equation (37) significantly differs from the Poisson distribution, which, as it is known, lead to power-law behavior of the imaginary part of inelastic scattering amplitude and, consequently, to the pole singularity of partial amplitude [5,14].

The described differences from a Regge theory are caused, apparently, by different physical mechanisms determing the inelastic scattering cross-section growth. In our model, a reduction of virtualities at the point of constrained maximum of inelastic scattering amplitude play a role of such mechanism. Consideration of similar diagrams in [2] lead to

$$\sigma_n \sim \frac{1}{n!}\frac{\ln^n(s)}{s^2} \tag{38}$$

At the same time a similar result is obtained in [15] by the calculating of phase space with "cutting" of transversal momenta, *i.e.* authors ignore the dependence of inelastic scattering amplitude on rapidity, and its role is reduced only to the cutting of integration over transversal momenta. Similar results are obtained in [5,14], where examined diagrams of same type, but with the exchange of Reggeons instead of virtual scalar particles was considered. In [5,14] as a result of approximation authors totally ignored the dependence of expression under the integral sign for cross-section on particle rapidity in the finite state, thus obtained results include the dependence on energy $\sqrt{s}$ only through the rapidity phase space. At the same time, as it evident from previous argumentations, the dependence of scattering amplitude on longitudinal momenta or rapidity is essential, because it is responsible for the certain mechanism of inelastic cross-sections growth and their sum.

Moreover, Equation (38) has positive derivative with respect to energy at sufficiently great *n* in sufficiently wide energy range. At the same time, sum of such expressions in [2] results in the cross-section, which decreases monotonically with energy growth. The reason for this may be apparent from Equation (38) factorial suppression of contributions with large *n*, which provide the positive contributions to derivative with respect to energy.

In the presented model such suppression disappears at transition from Equation (3) to Equation (6) due to taking into account diagrams, with different order of attachment of external lines to the "comb". The fact that the inclusion of such diagrams is essential as it seen from **Figure 10**, where the ratio of contribution $f_I^{(n)}\left(\sqrt{s}\right)$ from a diagram with the initial arrangement of momenta (see

Figure 2 in [1]) corresponding to the first summand in a sum Equation (30) to all sum $f_P^{(n)}\left(\sqrt{s}\right)$ is given.

As seen from **Figure 10** contribution from a diagram with the initial arrangement of external lines in the wide energy range is small fraction of the total sum Equation (30), which was natural to expect since sum Equation (30) has enormous number of positive summands. For the same reason, as was shown on **Figure 10**, the quota of contribution from a diagram with the initial arrangement of particles decreases sharply with increasing number of particles *n* in a "comb".

At the same time, as it follows from Equation (31), the growth of scattering amplitude at the maximum point related with the mechanism of reduction of virtualities can cause the growth of inelastic scattering cross-sections $\sigma_n'\left(\sqrt{s}\right)$ and, consequently, the growth of total cross-section. As an argument we can show results of numerical calculation of the function Equation (39), which are listed in **Table 1**.

$$Q_n\left(\sqrt{s}\right) = \frac{\left(A^{(0),n}\left(\sqrt{s}\right)\right)^2 J^{(0),n}\left(\sqrt{s}\right)}{\sqrt{s/4 - M^2}\sqrt{s}\left(M^2 + \left(P_{3\parallel}^{(0)}\right)^2\right)} \tag{39}$$

This function is the ratio of increasing amplitude at the maximum point to the multipliers, which "working" on lowering of the total cross-sections with energy growth.

Submitted data shows that the mechanism of virtuality reduction is "stronger" than multipliers, which "working" on lowering of the total cross-sections with energy growth.
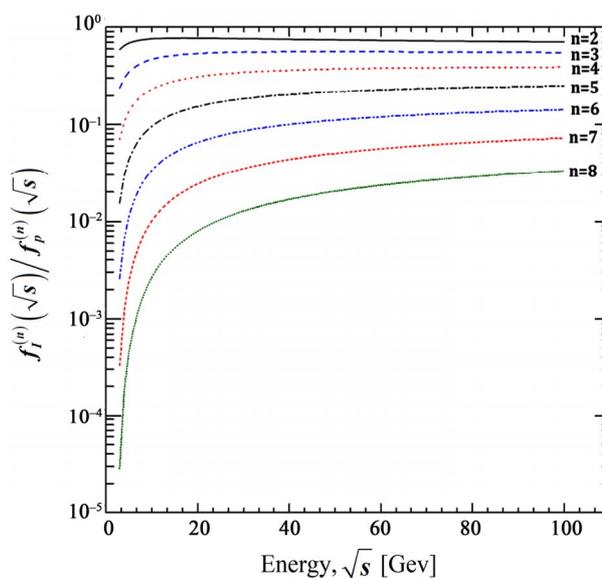

Figure 10. The ratio of the contribution from diagrams with an initial arrangement of the momenta $f_I^{(n)}\left(\sqrt{s}\right)$ to the sum of diagrams corresponding to all possible momenta arrangements $f_P^{(n)}\left(\sqrt{s}\right)$ at different *n*.

Table 1. Energy dependence of the function Equation (39) at n = 10 and n = 20.

$\sqrt{s}$, GeV	$\ln\left(Q_{10}(s)\right)$	$\ln\left(Q_{20}(s)\right)$
5	−68.867	−202.469
15	−48.936	−133.814
25	−44.874	−120.196
35	−43.036	−113.138
45	−41.993	−108.585
55	−41.328	−105.315
65	−40.874	−102.81
100	−40.065	−97.131
200	−39.622	−89.901
300	−39.74	−86.537
500	−40.191	−83.029
900	−41.043	−79.833
1800	−42.399	−77.008
5000	−44.905	−74.318
14,000	−47.862	−72.979

From Equation (33) follows that with increasing of *n* amplitude at the maximum point will increase sharply with energy growth. Thus, we can expect that factor $f_P^{(n)}\left(\sqrt{s}\right)$, which besides of $Q_n\left(\sqrt{s}\right)$ also inters into the expression of cross-section will decrease, but quite slowly. As is obvious from Equation (9), the possible decrease of $f_P^{(n)}\left(\sqrt{s}\right)$ is caused due to the fact that $f_P^{(n)}\left(\sqrt{s}\right)$ include the product of terms, corresponding to diagrams in which external lines with the same momenta can be attached to the different vertices of the diagram. As result, the momentum of such line cannot have a value that simultaneously set maximum for both vertices. Moreover, with energy growth distance between rapidities corresponding to particles, which providing maximum at the different vertices of the diagram, increase. This can lead to decreasing of value $f_P^{(n)}\left(\sqrt{s}\right)$ with energy. However, as it obvious from relations (see Equation (75) and Equation (81) [1]), we write them here:

$$y_{\frac{n}{2}} = \frac{1}{n+1}\operatorname{arccosh}\left(\frac{\sqrt{s}-n}{2M}\right) \qquad (40)$$

$$y_{\frac{n-1}{2}} = \frac{2}{n+1}\operatorname{arccosh}\left(\frac{\sqrt{s}-n}{2M}\right) \qquad (41)$$

the difference of these rapidities decreases with increase of particle's number on the diagram. Therefore, it is hoped that decrease of $f_P^{(n)}\left(\sqrt{s}\right)$, even if it will take place, will be not too sharp and cross-sections for high multiplicities of particles will also grow at least in the certain energy range. This will lead to the amplification of contributions with positive derivative with respect to energy into the total scattering cross-section.

As it follows from Equation (33), that at sufficiently high energies the amplitude at the maximum point tends to a constant value and mechanism of the reduction of virtualities become exhausted. This, however, can be avoided if we consider model in which the virtual particles on the diagram of the "comb" type are field quanta with zero mass. Then amplitude at the maximum point will tends to infinity at the infinite increase of energy. All computation in this case can be done similarly to what was described above. In this case, when calculating the first eight inelastic contributions in the wide range of energies does not give us contributions with negative derivative with respect to energy. Therefore we inclined to believe that such model can describe total cross-section growth to arbitrary large energies.

4. Conclusions

From demonstrated results it can be conclude that replacing of the "true" scattering amplitude associated to the multi-peripheral processes within the framework of perturbation theory by its Gaussian approximation is an acceptable approximation. The main conclusion is, that the mechanism of virtuality reduction (considered in [1]) may play a major role in ensuring the experimentally observed increase of the total cross-section [10,11], at least in some range of energies. This growth was obtained with allowance for σ_n at $n \leq 8$. However, as it follows from $\sigma_n'\left(\sqrt{s}\right)$ dependences, the maximum point of cross-section is shifted toward to higher energies with increase of *n*. We can therefore expect that in the consider energy range accounting of $\sigma_n'\left(\sqrt{s}\right)$ will add summands with positive derivative with respect to energy to expression for the total scattering cross-section, which leads to the fact that at least in the considered energy range obtained growth will only intensify.

Discussed above differences from the Reggeon theory suggest that our model is not a model of Reggeon with intercept high than unity and increase of the cross section is occurred in different way. This is also evident from the fact that in the model with a nonzero mass of virtual particles cross-section σ_n' at $\sqrt{s} \to \infty$ tends to zero. This is a consequence of the fact that the absolute value of virtualities cannot decrease indefinitely, because it is bounded below by zero. Therefore, for sufficiently low coupling constant, when for however-anything high multiplicities do not contribute to the total cross section, at sufficiently

high energies the total cross section should begin to decrease.

An additional conclusion is the necessity of accounting the sum of all diagrams with all the permutations of external lines for the scattering amplitude. Although with energy growth the fraction of contribution to the cross section of the diagram with an initial arrangement of the lines of the final particles increases and with $\sqrt{s} \to \infty$ will tends to unity. In a wide range of energies, this fraction is small and decreases with multiplicity increase, which can be easily understood on the basis of the positivity of the amplitudes in the multi-peripheral model.

Note that the application of Laplace method is not limited by simplest diagrams. Therefore, our goal is further consideration of the more realistic models using same method, especially in terms of the law of conservation of electric charge.

REFERENCES

[1] I. Sharf, G. Sokhrannyi, A. Tykhonov, K. Yatkin, N. Podolyan, M. Deliyergiyev and V. Rusov, "Mechanisms of Proton-Proton Inelastic Cross-Section Growth in Multi-Peripheral Model within the Framework of Perturbation Theory. Part 1," *Journal of Modern Physics*, Vol. 2, No. 12, 2011, pp. 1480-1506.

[2] D. Amati, A. Stanghellini and S. Fubini, "Theory of High-Energy Scattering and Multiple Production," *Il Nuovo Cimento* (1955-1965), Vol. 26, No. 5, 1962, pp. 896-954.

[3] I. G. Halliday, "Self-Consistent Regge Singularities," *Il Nuovo Cimento A* (1965-1970), Vol. 60, No. 2, 1969, pp. 177-184.

[4] E. A. Kuraev, L. N. Lipatov and V. S. Fadin, "Multi Reggeon Processes in the Yang-Mills Theory," *Soviet Physics—JETP*, Vol. 44, 1976, pp. 443-450.

[5] P. D. B. Collins, "An Introduction to Regge Theory and High Energy Physics," *Cambridge Monographs on Mathematical Physics*, Cambridge University Press, Cambridge, 1977. doi:10.1017/CBO9780511897603

[6] L. N. Lipatov, "Integrability Properties of High Energy Dynamics in Multi-Color QCD," *Uspekhi Fizicheskikh Nauk*, Vol. 174, No. 4, 2004, pp. 337-352. doi:10.3367/UFNr.0174.200404a.0337

[7] L. N. Lipatov, "Bjorken and Regge Asymptotics of Scattering Amplitudes in QCD and in Supersymmetric Gauge Models," *Uspekhi Fizicheskikh Nauk*, Vol. 178, No. 6, 2008, pp. 663-668.

[8] M. G. Kozlov, A. V. Reznichenko and V. S. Fadin, "Quantum Chromodynamics at High Energies," *Vestnik NSU*, Vol. 2, No. 4, 2007, pp. 3-31.

[9] N. G. De Bruijn, "Asymptotic Methods in Analysis," 1st Edition, Bibl. Matematica, Amsterdam, 1958.

[10] K. Nakamura and Particle Data Group, "Review of Particle Physics," *Journal of Physics G*: *Nuclear and Particle Physics*, Vol. 37, No. 7A, 2010, p. 075021. doi:10.1088/0954-3899/37/7A/075021

[11] G. Aad *et al.*, "Measurement of the Inelastic Proton-Proton Cross-Section at $\sqrt{s}$ = 7 TeV with the ATLAS Detector," *Nature Communication*, Vol. 2, 2011, p. 463. doi:10.1038/ncomms 1472

[12] A. Donnachie and P. V. Landsho, "Total Cross Sections," *Physics Letters B*, Vol. 296, No. 1-2, 1992, pp. 227-232. doi:10.1016/0370-2693(92)90832-O

[13] A. B. Kaidalov, "Pomeranchuk Singularity and High-Energy Hadronic Interactions," *Uspekhi Fizicheskikh Nauk*, Vol. 173, No. 11, 2003, pp. 1153-1170. doi:10.3367/UFNr.0173.200311a.1153

[14] Y. Nikitin and I. Rozental, "Theory of Multiparticle Production Processes," Harwood Academic Publishers, New York, 1988.

[15] E. Byckling and K. Kajantie, "Particle Kinematics," Wiley, London, 1973.